Journal of Applied Polymer Science

Combined puncture/cutting of elastomer membranes by pointed blades: Characterization of mechanisms

Ennouri Triki,[1] Phuong Nguyen-Tri,[1] Chantal Gauvin,[2] Meriam Azaiez,[1] Toan Vu-Khanh[1]

[1]Département Génie mécanique, École de Technologie Supérieure (ÉTS), 1100 Rue Notre-Dame Ouest Montréal, H3C 1K3, QC, Canada

[2]L'Institut de Recherche Robert-Sauvé en Santé et en Sécurité du Travail (IRSST), 505 de Maisonneuve Blvd West, Montréal, H3A 3C2, QC, Canada

Correspondence to: T. Ennouri (E-mail: ennouri.triki.1@ens.etsmtl.ca)

ABSTRACT: The simultaneous puncture and cutting behavior of elastomers was investigated by pointed blades. Puncture/cutting tests by three-pointed blades were performed with different elastomer membranes, including butyl, neoprene, and nitrile rubbers. The fracture mechanisms associated to puncture/cutting were investigated. The quantitative material properties which control the puncture/cutting resistance are obtained. The results have showed that the crack growth propagation is controlled by the material viscoelastic and the fracture behaviors of material, as well as the friction between the pointed blade and material. As evidenced from the fracture mechanism analysis, the friction contributes to the resistance of material against the simultaneous puncture and cutting by a factor of more than 60%. It has also been that the penetration force and the global fracture energy depend on the blade tip angle, the cutting edge angle, and the blade lubrication. Finally, an analysis of mixed-mode fracture based on puncture/cutting by pointed blades has been described. The crack propagation is a synergistic interaction between the fracture modes I and III. © 2015 Wiley Periodicals, Inc. J. Appl. Polym. Sci. **2015**, *132*, 42150.

KEYWORDS: elastomers; membranes; mechanical properties; theory and modeling

Received 17 November 2014; accepted 25 February 2015
DOI: 10.1002/app.42150

INTRODUCTION

Puncture-resistant materials for protective gloves are required for a range of several industrial sectors, especially workplaces exposed to knife tips, metal sharps, or glass splinters. Lacerations of cut and puncture types cause more than 50% of hand injuries according to various sources.[1–3] However, the appropriated protective gloves against these hazards are not yet available up to now. Therefore, resistance to puncture by pointed blades is considered a relevant mechanical property of materials used in protective gloves. The development of materials having a high protection level for the puncture by pointed objects requires a better understanding of the puncture and cutting mechanisms. Various investigations of puncture and cutting have been performed on specific cases involving different protective materials. In some cases, new test methods have been proposed.

The puncture by normalized probes and cutting by a razor blade are already published in the literature.[4–11] Several test methods have been adopted by ISO or by ASTM to characterize the resistance of protective gloves to cutting and to puncture.[12–15] These test methods are designed for several types of protective materials, including elastomer membranes, coated fabrics, and textiles. It has been suggested that the puncture resistance can be obtained through the measurement of the penetration force, which equals to the maximal value of force curve. In the case of cutting, the cutting force has been reported to correspond to blade displacement of 20 mm.

The cut resistance of elastomer materials can be affected by two mechanisms: the viscoelastic behaviour of material and the contribution of the friction between the blade and the material.[9,16] The friction contributes significantly to the cutting energy. The puncture tests by a rounded probe showed that the penetration force largely depends on the deformation of elastomer membranes.[8,17] However, in the case of puncture by medical needles,[17–19] the material deformation is low. A linear relationship between the penetration force and probe (medical needles and conical and rounded probes) diameter is observed.[17]

From a fundamental point, the mechanisms of the simultaneous puncture and cutting of elastomer membranes are still not largely explored. It should be noted that no fundamental understanding of the mechanisms controlling the puncture/cutting for

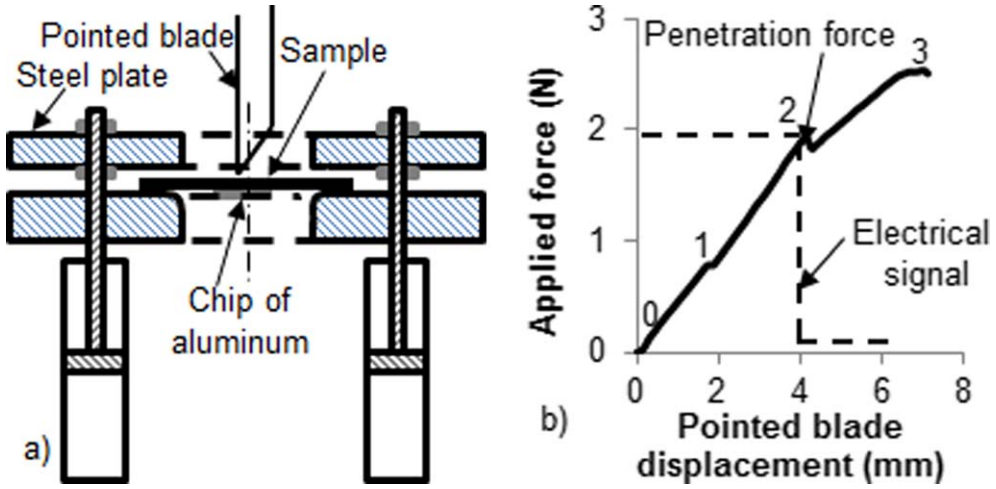

Figure 1. (a) Experimental measurement setup, (b) Typical force-displacement curve. [Color figure can be viewed in the online issue, which is available at wileyonlinelibrary.com.]

elastomer membranes is investigated. However, in the case of textile composites, various practical studies have been performed to evaluate the resistance to stab knife.

Gong *et al.*[20] studied the fracture resistance of various layers of Kevlar fabric by a stab knife. The fracture resistance is evaluated by both the calculations of the impact energy and the penetration depth of knife in the material. The results showed that the puncture/cutting resistance is highly depended on the inter-yarns friction and the number of fabric layers. Therefore, the higher puncture/cutting resistance of woven aramid fabric is observed with thin laminated films.[21] Alternative finite element analyses of stab knife on composite materials have been also performed.[22] The knife penetration force of material is influenced by the yarn rigidity and yarn static friction. Other results showed that the penetration force of composite materials is highly depended on the sharp blade geometry.[23] Two parameters: the cutting resistance without deformation of material and the shear force of fibers account for the creation of a new fracture surface.

The ultimate goal of this article is to propose a new approach to evaluate the resistance of elastomer membranes to pointed blades. The mechanisms responsible for the puncture/cutting process are determined. The effects of blade lubrication, pointed blade geometry, and cutting edge angle will be investigated. An analysis of the synergy between puncture and cutting processes is also discussed.

EXPERIMENTAL

Materials and Pointed Blades

Tests were performed on three different elastomer membranes (McMaster Carr. Ltds.): neoprene rubber (1.6- and 3.2-mm thick), nitrile rubber (0.4-, 0.8-, 1.6-, and 3.2-mm thick), and butyl rubber (1.6-mm thick). These polymers are commonly used in the manufacturing of protective gloves.

Three models of pointed blade with different tip angles have been used to perform the puncture/cutting tests. The first blade was a fine blade with a 22.5° tip angle (X-Acto, Model X211). The second one was a medium blade with a 35° tip angle (X-Acto, Model X224). The third one was a large blade with a 56° tip angle (X-Acto, Model X219).

Puncture/Cutting Process by a Pointed Blade

Force Measurement. The puncture tests by pointed blades were performed using a test method similar to ASTM F1342-05 standard test method.[14] The material sample was clamped between two steel plates having 38 mm diameter holes [Figure 1(a)] to let the sample deform freely during the test. The pointed blade was positioned perpendicularly to the sample in a mechanical test frame machine (Alliance STM) equipped with a 25-N load cell. The test consists in moving down the blade at a constant displacement rate of 100 and 250 mm/min against the sample. The applied force is recorded with the pointed blade displacement. As shown in Figure 1(b), the force-displacement curve displays several peaks. To identify the peak corresponding to the penetration force at which the blade tip reaches the underside of the membrane, a thin film of aluminum was fixed underneath of the sample and coupled with the pointed blade by wire, to detect the blade tip by electrical contact.

Global Fracture Energy and Friction Energy Measurements. The global fracture energy and the global friction energy, which are responsible of the creation for a new fracture surface in rubber materials, were measured by loading/unloading test at 100 mm/min (Figure 2). These types of test are commonly used in several breaking methods to characterize the fracture energy.[18,19,24–26] Rivlin and Thomas proposed this approach to calculate the tearing energy of rubbers.[26] This approach was also used to study the tearing energy of textile materials by trouser tear tests and tensile tests.[27] Others studies have characterized the puncture and cutting of rubber by loading/unloading tests.[18,19,24,25]

In this work, loading/unloading test were performed at various applied pointed blade displacement values. The first step is moving down the pointed blade through the sample, *i.e.*, a maximum of the applied blade displacement is reached (loading, step 1, Figure 2), and then pull out the blade from the sample (unloading, step 2). Therefore, similar tests without crack propagation were performed on the same puncture/cutting sample (reloading, steps

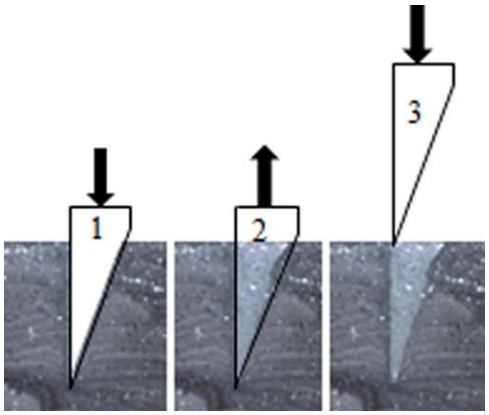

Figure 2. Example of measured of fracture and friction forces of the same material and pointed blade, (1) Loading test: Puncture/cutting test, (2) Unloading test: extraction of blade, (3) Reloading test: Sliding blade in fracture surface (10X magnification). [Color figure can be viewed in the online issue, which is available at wileyonlinelibrary.com.]

3 and n°2), *i.e.*, the pointed blade is slipped inside the fracture surface to evaluate the contribution of friction.

These test cycles helps to characterize the global friction energy and the global fracture energy. For each loading/unloading/reloading test cycle, two curves of fracture and friction tests were recorded at a pointed blade displacement of 7 mm, as shown in Figure 3. The global friction energy $U_{Friction}$ and the global fracture energy $U_{Fracture}$ were calculated from the eq (1).

$$U_{Fracture(Friction)} = \int F_{Fracture(Friction)}\, dl \quad (1)$$

Where $F_{Fracture}$ and $F_{Friction}$ are respectively the fracture and the friction forces measured at a pointed blade displacement l.

The previous experimental formalism was used to evaluate the contribution of friction and fracture energies in puncture/cutting process. As shown in Figure 3, the puncture/cutting energy U_{Total} can be given by eq. (2).

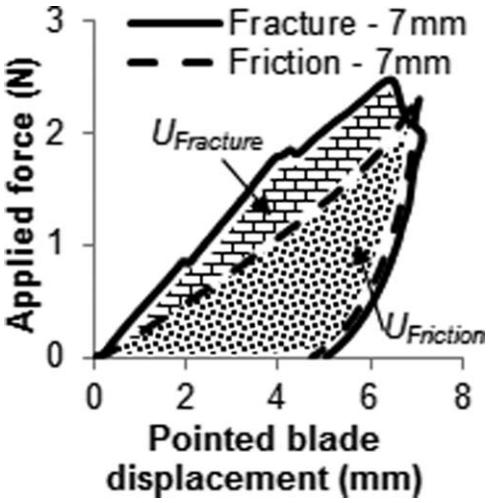

Figure 3. Typical loading/unloading force–displacement curves of puncture/cutting test and friction test with a 7 mm applied pointed blade displacement.

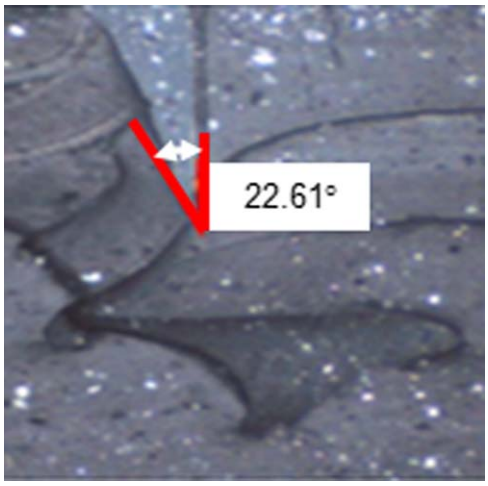

Figure 4. Fracture surface created by a pointed blade (20× magnification). [Color figure can be viewed in the online issue, which is available at wileyonlinelibrary.com.]

$$U_{Total} = U_{Fracture} + U_{Friction} \quad (2)$$

The fracture surface was measured to understand the crack growth mechanisms. As the loading/unloading/reloading tests were completed, the specimen was opened by a special cutter to separate the two created crack faces. The crack face was then observed in the underformed state of sample using an optical microscopy. The fracture surface is triangular as the shape of the pointed blade (Figure 4).

Effect of Experimental Conditions. The pointed blade was wetted by thin layer of a metalworking fluid to study the lubrication effect. The penetration force and the friction and fracture energies of non-lubricated blades are also inserted for reference.

In industrial working places, various attack angles between pointed blades and protective material are possible. Thus, the effect of this parameter on penetration force was investigated. The setup used for measuring the simultaneous puncture and cutting resistance was oriented to several sample angles ($\alpha = 0°$, 3°, 5°, 8°, and 11°) (Figure 5). The penetration force was recorded in two orientations, X and −X, of the cutting edge of 35° and 56° tip angles pointed blades.

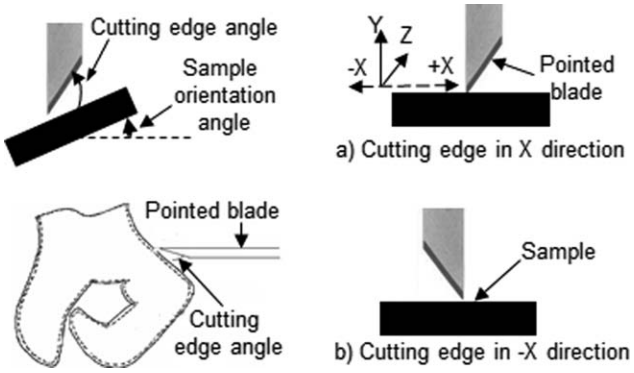

Figure 5. Schematic representation of several setup orientation angles, (a) cutting edge blade oriented in X direction, (b) cutting edge blade oriented in -X direction.

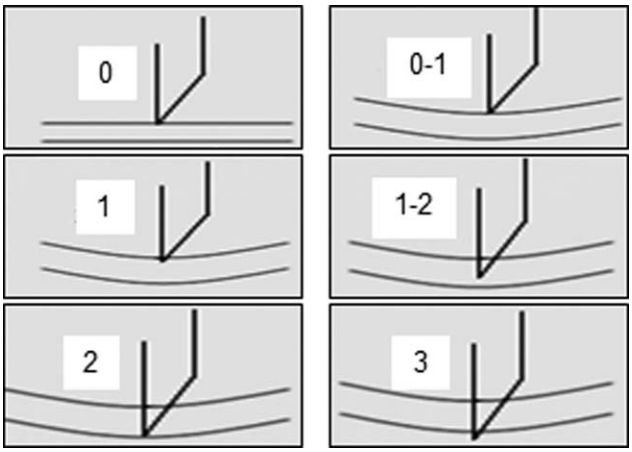

Figure 6. Pictures of the puncture/cutting steps of elastomer membranes by a pointed blade.

RESULTS AND DISCUSSION

Fracture Mechanisms

Figure 1(b) displays the variation of the applied force as a function of pointed blade displacement for the neoprene membrane (1.6 mm thick) and blade of 22.5° tip angle. Three peaks (peak n°1, n°2, and n°3) and four inflection points, which characterize the puncture/cutting behavior of material (0–1, 1–2, 2–3, and 3–4), are observed. The pointed blade gradually penetrates in the material and produces crack growth propagation by simultaneous puncture and cutting (Figure 6). The friction between the pointed blade and material is continuously contributed during the puncture/cutting process.

The first part (0–1) corresponds to the resistance to viscoelastic deformation of elastomer membrane. At position n°1 [Figure 7(a)], the deformation of material reaches a maximum and then the blade tip begins to penetrate gradually into the membrane (pointed blade displacement $>$ 2 mm). This position corresponds to the first increment of crack growth propagation. The change in the shape of applied force curve is related to the viscoelastic behavior of material. It appears that the viscoelastic behavior affects notably to the crack growth propagation process.

Between positions n°1 and n°2 [Figure 7(b)], the pointed blade continues to penetrate gradually in the material and produces a crack by the simultaneous puncture and cutting processes. Because the pointed blade remains in contact with material, the friction plays a continuous role with respect to the puncture/cutting process. The applied force has not yet reached the position n° 2 (applied force $<$ 1.95 N), *i.e.*, the pointed blade is not in contact with the lower face of elastomer membrane. However, the applied force is reached the position n°2, whereas the pointed blade is in contact with the lower face of the sample. From position n°2 ($>$ 1.95 N), the pointed blade completely crosses the lower face of elastomer membrane. Therefore, the applied force continues to increase [Figure 7(c)].

When the pointed blade passes through the sample, the applied force reaches to another peak (position n°3) [Figure 7(d)]. The crack growth propagation is only assumed by the cut and friction forces. For this reason, the applied force is almost constant as the shape of the force curve obtained during the cutting by a razor blade.[7,28–30] Therefore, the fracture process is largely controlled by the friction in the cutting edge of the pointed blade. According to the previous results, the large contributions of the viscoelastic behavior and the friction between material and pointed blade make them good candidates for the puncture/cutting resistance materials.

Effect of Lubrication

An investigation of the effect of blade lubrication on the puncture/cutting process shows a significant reduction of the resistance to puncture/cutting by lubricated blade. As it can be seen in Table I, a decrease of penetration force (approximately 50%) was recorded with neoprene and nitrile rubber membranes punctured by a lubricated blade of 35° tip angle. This result can be attributed to the difference in the contribution of puncture/cutting mechanisms for lubricated blade compared with nonlubricated blade. The lubrication of pointed blade is eventually leading to a reduction of friction during the puncture/cutting process. The later will be investigated in the next section. The effect of blade lubrication was also examined with the global fracture energy and global friction energy at a pointed blade displacement of 7 mm (Table II). The values of the energies obtained with lubricated and nonlubricated blades of three blade tip angles were compared. The obtained result clearly indicates a reduction of the global fracture energy of neoprene rubber with the lubricated blades. The similar trend was observed in the case of the variation of the value of the penetration force as a function of lubrication effect (Table I). This effect can be attributed to the friction contribution. As shown

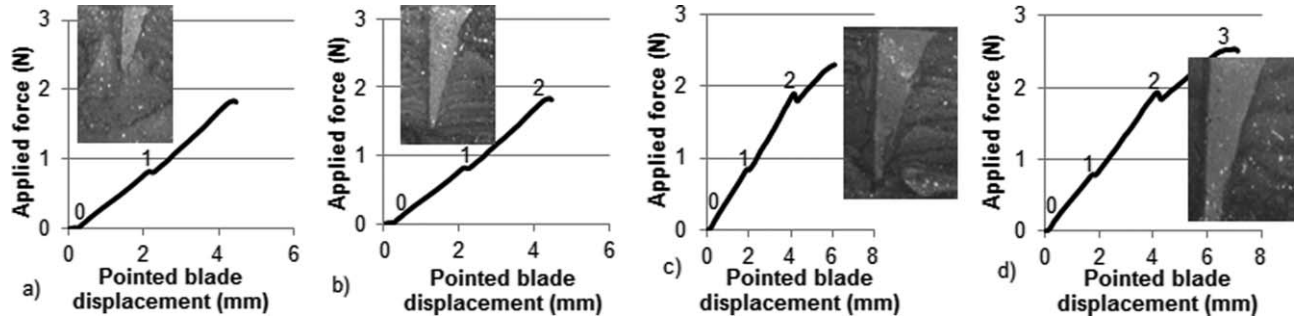

Figure 7. Typical force–displacement curves for puncture/cutting by a pointed blade of 22.5° and fracture surfaces created into a neoprene rubber membrane (1.6-mm thick).

Table I. Comparison of Penetration Force Values Obtained at Displacement Rate of 250 mm/min

Material	Thickness (mm)	Condition	Penetration force (N)
Neoprene	1.6	Nonlubricated	3.42 (0.09)
		Lubricated	2.49 (0.03)
	3.2	Nonlubricated	11.03 (1.22)
		Lubricated	6.69 (0.35)
Nitrile	1.6	Nonlubricated	5.31 (0.25)
		Lubricated	3.84 (0.29)

in Table II, a significant decrease of the global friction energy can be obtained with lubricated blade. Therefore, the presence of a lubricant does not completely remove the friction force between the blade and elastomer membrane.

Contribution of Friction

The relationship between the combined mechanisms of friction and fracture was investigated to quantify the contribution of friction to the puncture/cutting process (Figure 3). This friction dissipation at crack propagation involves two friction phenomena.[9] The first one is associated with the lateral pressure of crack tip surfaces on both sides of pointed blade. The second phenomenon is due to the tangential contact between cutting edge of blade and material.

As shown in Figure 3, a minor difference between the maximum friction force and the maximum fracture force is observed. Because of that, the relationship between the both maximum forces should not be used to characterize the friction contribution. On the other hand, the global friction energy U_{Friction} is higher than the global fracture energy U_{Fracture}. The U_{Friction} represents about two-third of the U_{Total}. The similar finding has been reported in the case of elastomer cutting by a razor blade.[9] Quantitatively, the global cutting energy dissipates to cut a neoprene rubber basically derives from the friction force. In addition, viscoelastic behavior of elastomer membranes can affect the friction and the fracture energies.[31–33] It has been shown that the cutting energy with or without friction includes a viscoelastic contribution. Figures 6 and 7 revealed that the elastomer membrane is deformed by the linear viscoelastic behavior, before initial crack growth occurs. This fundamental property has not eventually a significant effect on the puncture/cutting behavior, because of the continuous cutting edge of the pointed blades.

To confirm the friction contribution, the global friction energy was measured with several nitrile and neoprene rubber membranes punctured by the three lubricated and nonlubricated pointed blades. The results in Figure 8 allow us to prove that the friction contribution to the puncture/cutting resistance is almost constant with several puncture/cutting cases. It can also be seen from this graphic that the relationship between the global friction energy and the global fracture energy is almost constant and all data point out the independent of the friction contribution to the test conditions. Therefore the U_{Friction} increased by a factor of 2.45 with the increasing of the U_{Fracture} for all experimental cases. Thus, it believes that the puncture/cutting process of elastomers by a pointed blade is largely controlled by the friction phenomenon.

Effect of Blade Tip Angle

An investigation of the variation of the penetration force as a function of the blade tip angle (22.5, 35, and 56°) was performed with nitrile and butyl rubber membranes of 1.6-mm thick (Table III). An increase in the penetration force with the blade tip angle is observed. The results could be attributed to the increase of the tip angle, which in turn leads to an increase of the friction as the contact surface between the blade and material increases.

Table II shows the effect of blade tip angle on the global fracture energy for a neoprene rubber membrane of 1.6-mm thick. This global energy strongly increases with the decrease of blade acuteness (increase of blade tip angle). The overall shape of this trend is similar to that of the penetration force. The fracture modes of material and the friction contribution can be given here for explanation.

The crack associated to the puncture by pointed blades of tip angle between 22.5° and 56° is monitored by fracture mixed-modes (Figure 9). There are two fracture modes (mode I + III) that can interfere in this process. The puncture with the acuteness blades promotes the fracture mode III, *i.e.*, the crack tip opening displacement, which performed by the shear stress, is parallel with the crack tip face. The crack propagates at high speed to create a new fracture surface and the pointed blade rapidly penetrates into the material. By comparison, in the case of the pointed blade with tip angle around of 90°, the crack growth can be manifested by the fracture mode I. This crack growth propagation is assumed by the normal stress that is perpendicular with the crack propagation plane. In this case, the crack propagation is relative low and the crack growth occurs more proucely in a superficial surface of the sample.

Effect of Cutting Edge Angle

The effect of cutting edge angle on the completely penetration force is displayed in Figure 10. For the two pointed blades of

Table II. Comparison of the Global Friction Energy and the Global Fracture Energy Obtained at Displacement Rate of 100 mm/min

	Global fracture energy (N.mm)		Global friction energy (N.mm)	
Blade tip angle (°)	Nonlubricated	Lubricated	Nonlubricated	Lubricated
22.5	4.05 (0.21)	3.55 (0.25)	6.02 (0.08)	4.15 (0.11)
35	6.15 (0.05)	4.2 (0.06)	12.18 (1.01)	5.55 (0.06)
56	8.12 (0.04)	6.2 (0.09)	16.22 (0.49)	8.6 (0.13)

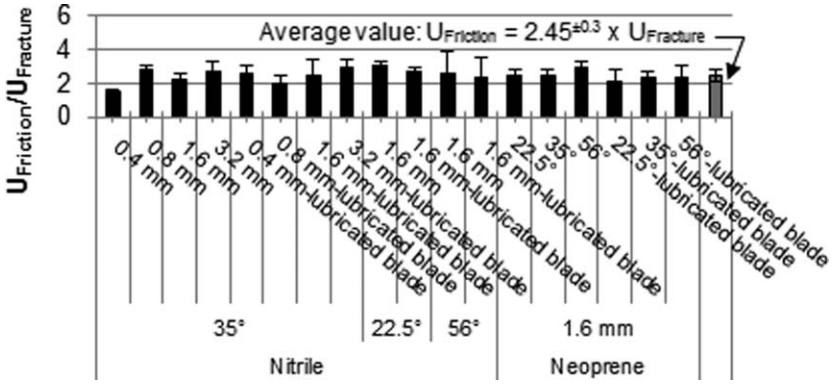

Figure 8. Comparison of the $U_{Friction}$ and the $U_{Fracture}$ values of several puncture/cutting tests at displacement rate of 100 mm/min.

35° and 56°, the curve, which describes the relationship between the penetration force and cutting edge angle, are well superimposed on a single master curve. The penetration force abruptly decreased with increasing of the cutting edge angle. The shape of master curve is similar to both neoprene rubber membranes of 1.6- and 3.2-mm thick. In accordance with the puncture/cutting results obtained with large cutting edge angles or acuteness blades, the effect of cutting edge angle on penetration force appeared similarly to the effect of blade tip, as illustrated in Table III. When the cutting edge angle is close to 90°, *i.e.*, a blade of fine tip angle, a lower value of the penetration force is observed. The puncture/cutting process is assumed by the fracture mode III. Otherwise, both the small cutting edge angles and blades of large tip angles can give the same puncture/cutting process. Indeed, a high value of the penetration force is obtained (Figure 10). Therefore, the crack propagation is eventually controlled by the fracture mode I.

Discussion About the Difference in Fracture Mechanisms Between Pointed Blades, Probes and Medical Needles

It has been reported in the case of puncture of elastomer membranes by conical probe that the fracture mechanism is controlled by the maximum deformation of material.[18] Another investigation on the cutting of rubber material by a razor blade reported a large contribution of friction to the fracture energy.[9] However, in the case of puncture by medical needle, the contribution of friction played a minor role toward the fracture of material.[17] The puncture/cutting process has shown the simultaneous contribution of friction and viscoelastic behavior, during the crack propagation. The material deformation by pointed blades is much lower than that observed with spherical and conical probes.

To compare the penetration force of puncture/cutting with that of probes and medical needles,[9,17,23] the results are illustrated together in Table IV. The penetration force value for puncture by a pointed blade is equal to twice of penetration force associated to the puncture by a medical needle, but it's lower than that recorded with conical probe. The results can be related to the crack propagation modes.[17,18] The crack tip diameter is controlled by tip diameter of probes[26] (conical probe, medical needle, and pointed blade). Indeed, the crack tip radius of

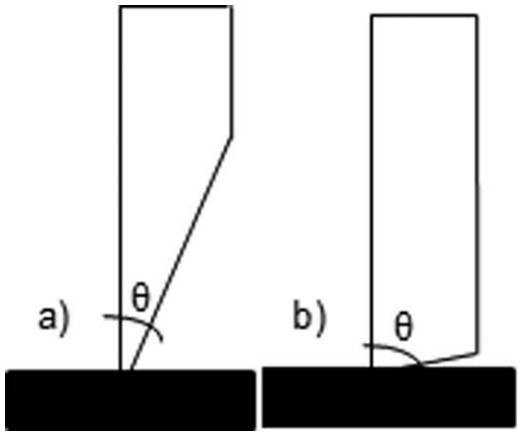

Figure 9. Fracture mixed mode I+III, (a) crack growth dominated by shear stress (mode III), (b) crack growth dominated by normal stress (mode I).

Table III. Variation of the Penetration force as a Function of Blade tip Angle Obtained at Displacement Rate of 250 mm/min for the Sample of 1.6 mm-thick

	Penetration force (N)	
Blade tip angle (°)	Butyl	Nitrile
22.5	6.01 (0.33)	3.42 (0.26)
35	13.65 (0.34)	6.09 (0.37)
56	17.03 (0.56)	9.23 (0.09)

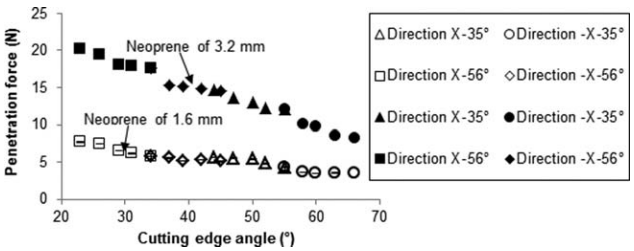

Figure 10. Variation of penetration force as function of cutting edge angle obtained at displacement rate of 250 mm/min.

Table IV. Comparison of the Values of the Penetration force of the Conical Probe, the Medical Needle and the Pointed Blade for Neoprene (1.6 mm-thick) Obtained at Displacement Rate of 100 mm/min[9]

Type of aggressors	Penetration force (N)
Conical probe	19.2 (0.5)
Medical needle	2.2 (0.1)
Pointed blade	3.8 (0.5)

pointed blade is bigger than that created by medical needle and smaller than the crack tip associated to conical probe.

Puncture/Cutting Process

An analysis of the puncture/cutting process is proposed to describe the crack propagation in elastomer materials (Figure 11). Two crack growth processes are observed during the puncture by pointed blades. The first is the puncture in the normal direction. The second is the cutting process, which is occurred in the tangential direction. It seems that the change of blade tip angle affects the fracture mode of material and consequently modifies the puncture process and cutting process contributions. When the blade tip angle is acute (for example 22.5°), the crack growth propagation created by puncture process and by shear stress is dominated. The crack depth is therefore superior to the crack length in tangential direction [Figure 11(a)]. In addition, a major rule of cutting-process and normal stress is revealed with the puncture/cutting occurred with larger blade tip angles (for example $\geq 56°$). As a result, the cut length is greater than the puncture depth [Figure 11(c)].

Contribution of Friction and Fracture Forces

An analysis of the distribution of puncture/cutting forces is performed to provide a better explanation with respect to the fracture mechanic and mechanisms associated to a puncture/cutting by pointed blades. Figure 12 shows that the penetration force includes both normal and tangential forces. According to the

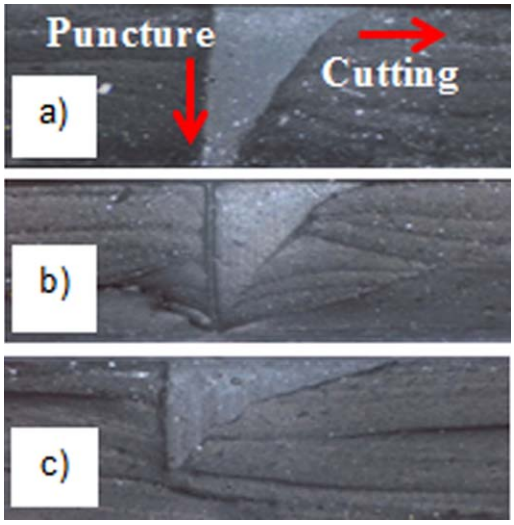

Figure 11. Fracture surfaces obtained with various pointed blades of: (a) 22.5°, (b) 35°, and (c) 56°. [Color figure can be viewed in the online issue, which is available at wileyonlinelibrary.com.]

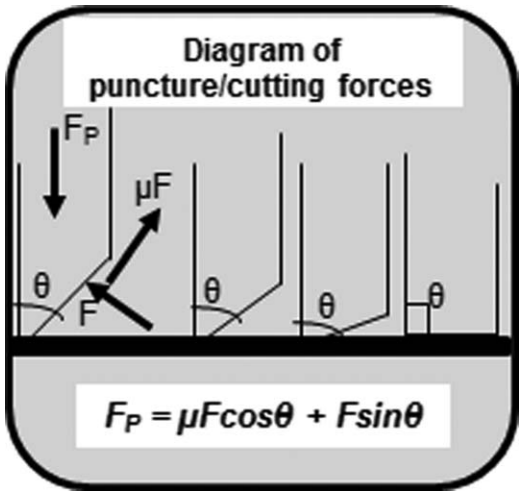

Figure 12. Diagram of the distribution forces during the puncture/cutting test by pointed blades for elastomer membrane.

fracture mixed mode, the penetration force in equilibrium can thus be expressed by eq. (3).

$$F_P = \mu F\cos\theta + F\sin\theta \quad (3)$$

Where F_P is the penetration force, μ is the coefficient of friction, θ the blade tip angle, and F is the result of the response to the applied normal force F_B, including fracture of material and the pressure of surfaces crack tip parameters.

The analysis of distribution forces clearly confirms that the friction force is mostly responsible for the crack growth propagation and puncture/cutting resistance. As it can be seen here, an increase of blade tip angle causes a decrease in the friction force $\mu F\cos\theta$. However, an increase of the friction because of the lateral pressure of material on the both sides of blade is observed (Table II). As a consequence, the resistance associated to puncture/cutting is the highest. The distribution of puncture/cutting forces is proposed by eqs. (4–6).

$$\theta \rightarrow 90° \quad (4)$$

$$\mu F\cos\theta \rightarrow 0 \quad (5)$$

$$F_p \rightarrow F \quad (6)$$

On the other hand, the puncture/cutting test with the acuteness blade, as low blade tip angles or high cutting edge angles, shows a maximum value of friction force $\mu F\cos\theta$ at the cutting edge blade. Consequently, the penetration force exhibits a minimum value (Figure 10). Hence, the puncture/cutting forces are in the form:

Since$\theta \rightarrow 0°$, value of $\mu F\cos\theta$ is the highest value. Also, the maximum penetration force F_p has a tendency to $\mu F\cos\theta$. Indeed, the resistance to puncture/cutting is the lowest value.

CONCLUSION

In this work, the fracture mechanic and mechanisms of the simultaneous puncture and cutting associated to pointed blades have been investigated.

Our results show that the puncture/cutting of elastomer membranes is controlled by a macroscopic friction. The friction

between pointed blade and material significantly contributed to the crack growth propagation. The puncture/cutting energy includes more than 60% of friction contribution. A decrease of penetration force, global fracture energy and global friction energy was also observed with the lubricated pointed blades. A similar finding was obtained with the effects of the cutting edge angles and the blade tip angles on the same mechanical properties. This result can be associated to the fracture mixed-modes and the contribution of friction.

The puncture by acuteness blade shows a domination of shear stresses and puncture-process. The crack is more propagated in the normal direction. The friction between blade cutting edge and material achieves a maximum value. The cutting-process, which is assumed by normal stress, is dominated during the puncture/cutting tests by a large blade tip angles. The friction between blade cutting edge and material is rather small. Therefore, the resistance to puncture/cutting is much higher than that observed in the case of acuteness blades.

ACKNOWLEDGMENTS

The authors are grateful to the Institut de recherche Robert-Sauvé en santé et en sécurité du travail (IRSST) for financial support of this work.

REFERENCES

1. Caple, D. Evaluation of Cut Resistance Gloves in the South Australian Meat Industry. *South Australia WorkCover Corporation, Adelaide* **2000**; p 25.
2. Commission de la santé: de la sécurité du travail (Québec Occupational Health et Safety Commission), deposit of central and regional data, data base of 2009 to 2011, Data processing by the IRSST: Montréal, **2014**.
3. Sorock, G. S.; Lombardi, D. A.; Peng, D. K.; Hauser, R.; Eisen, E. A.; Herrick, R. F.; Mittleman, M. A. *J. Occup. Environ. Hyg.* **2004**, *1*, 182.
4. Nguyen, C. T.; Vu-Khanh, T.; Lara, J. *Theor. Appl. Fract. Mech.* **2004**, *42*, 25.
5. Nguyen, C. T.; Vu-Khanh, T. *J. Mater. Sci.* **2004**, *39*, 7361.
6. Yang, Y.; Ponting, M.; Thompson, G.; Hiltner, A.; Baer, E. *J. Appl. Polym. Sci.* **2012**, *124*, 2524.
7. Lara, J.; Nelisse, N. F.; Cote, S.; Nelisse, H. J. *J. ASTM Int.* **1992**, *4*, 26.
8. Lara, J. Développement d'une méthode d'évaluation de la résistance à la perforation des gants de protection; *Rapport IRSST: Montréal* **1992**; R-059.
9. Vu-Khanh, T.; Vu Thi, B. N.; Nguyen, C. T.; Lara, J. Gants de protection : étude sur la résistance des gants aux agresseurs mécaniques multiples; *Rapport IRSST: Montréal* **2005**; R-424.
10. Cho, K.; Lee, D. *J. Polym. Sci. Part B: Polym. Phys.* **1998**, *36*, 1283.
11. Nguyen, C. T.; Dolez, P. I.; Vu-Khanh, T.; Gauvin, C.; Lara, J. *J. ASTM Int.* **2010**, *7*, 16.
12. ASTM F1790. Standard Test Method for Measuring Cut Resistance of Materials Used in Protective Clothing; Annual Book of ASTM Standards: West Conshohocken, PA, 2005; Vol. 11.03, pp 1602.
13. ISO13997. Protective Clothing, Mechanical Properties, Determination of Resistance to Cutting by Cutting Objects: Geneva, 1999; p 11.
14. ASTM F1342-05. Standard Test Method for Protective Clothing Material Resistance to Puncture; Annual Book of ASTM Standards: West Conshohocken, PA, **2005**; Vol.*11.03*, pp 1489.
15. ASTM F2878. Standard Test Method for Protective Clothing Material Resistance to Hypodermic Needle Puncture; Annual Book of ASTM Standards: West Conshohocken, PA, **2010**; Vol. *11.03*, pp 1.
16. Lara, J.; Turcot, D.; Boutin, J.; Daigle, R. La résistance des gants à la coupure -Développement d'une méthode d'essai; *Rapport IRSST: Montréal* **1995**; *R-103.*
17. Vu-Khanh, T.; Dolez, P. I.; Nguyen, C. T.; Gauvin, C.; Lara, J. Résistance des gants à la piqûre par les aiguilles Mise au point d'une méthode d'essai; *Rapport IRSST: Montréal* **2011**; *R-711.*
18. Nguyen, C. T.; Vu-Khanh, T.; Dolez, P. I.; Lara, J. *Int. J. Fract.* **2009**, *155*, 83.
19. Nguyen, C. T.; Vu-Khanh, T.; Dolez, P.; Lara, J. *Int. J. Fract.* **2009**, *155*, 75.
20. Gong, X.; Xu, Y.; Zhu, W.; Xuan, S.; Jiang, We; Jiang, Wa *J. Compos. Mater.* **2013**, *0*, 1.
21. Jessie, B.; Mayo, Jr.; Eric, D. W.; Mahesh, V. H.; Shaik, J. *Int. J. Imp. Eng.* **2009**, *36*, 1095.
22. Wang, L.; Zhang, S.; Gao, W. M.; Wang, X. *Compos. Model. Eng. Sci.* **2007**, *20*, 11.
23. Ankersen, J. Quantifying the Forces in Stabbing Incidents, Ph.D. Thesis, Ballistics and Impact Group, Department of Mechanical Engineering, University of Glasgow, Scotland, **1999**; Chapter *3*, p 67.
24. Felbeck, D. K.; Atkins, A. G. Strength and Fracture of Engineering Solids, 2nd ed.; Prentice Hall, **1995**; p 535.
25. Lake, G. J.; Yeoh, O. H. *J. Polym. Sci.* **1987**, *25*, 1157.
26. Rivlin, R.S.; Thomas, A. G. Beitsh Rubber Producer's Research Association, Welwy Garden City, Herts, England, **1953**, p 291.
27. Ennouri, T.; Patricia, D. I.; Vu-Khanh, T. *Compos. Part B* **2011**, *42*, 1851.
28. Vu, T. B. N.; Vu-Khanh, T.; Lara, J. *J. ASTM Int.* **2005**, *2*, 399.
29. Vu, T. B. N.; Vu-Khanh, T.; Lara, J. *J. Therm. Compos. Mater.* **2005**, *18*, 23.
30. Vu, T. B. N.; Vu-Khanh, T.; Lara, J. *J. Theor. Appl. Fract. Mech.* **2009**, *52*, 7.
31. Vu-Khanh, T. *J. Theor. Appl. Fract. Mech.* **1998**, *29*, 75.
32. Vu-Khanh, T.; Liu, B. *J. Reinf. Plast. Compos.* **1999**, *18*, 1087.
33. Cho, K.; Lee, D. J. *Polym. Sci. Part B: Polym. Phys.* **1998**, *36*, 1283.